Opto-Electronic Advances

Supplementary information

2021, Vol. 4, No. 1

DOI: 10.29026/oea.2021.200072

Plasma and nanoparticle shielding during pulsed laser ablation in liquids cause ablation efficiency decrease

Sarah Dittrich, Stephan Barcikowski* and Bilal Gökce

Technical Chemistry I and Center of Nanointegration Duisburg Essen (CENIDE), University of Duisburg-Essen, Universitaetsstr. 7, 45141 Essen, Germany.

*Correspondence: S Barcikowski, E-mail: stephan.barcikowski@uni-due.de

This file includes:

Supplementary information for this paper is available at https://doi.org/10.29026/oea.2021.200072

Section 1: Figure S1–Figure S3

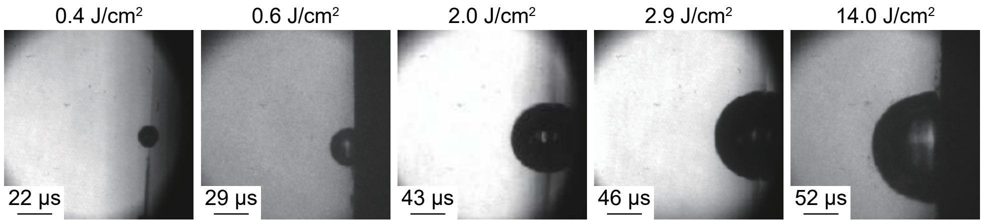

Fig. S1 | Maximal cavitation bubble extensions observed with a 1 ns laser system at the respective laser fluences; the scale bar equals 250 μm. The respective delay time is given in each image.

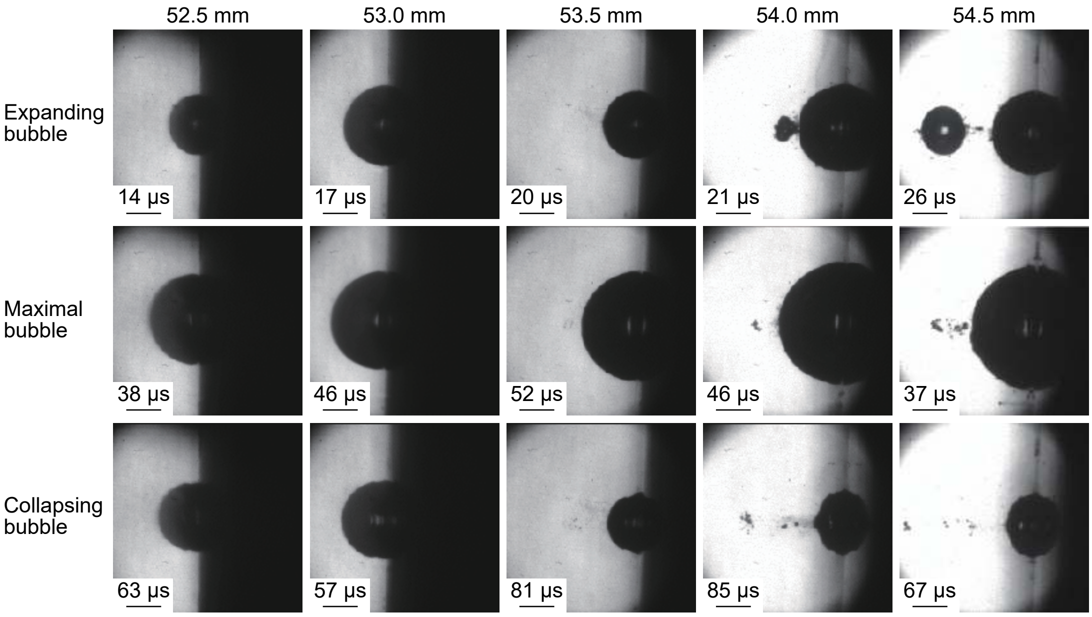

Fig. S2 | Exemplary cavitation bubbles at different distances between the target surface and the focusing lenses, i.e., different focal distances, during the expansion, the maximal extension, and the shrinking phase; the scale bar equals 250 μm. All images are obtained with a fluence of 14 J/cm². The respective delay time is given in each image.

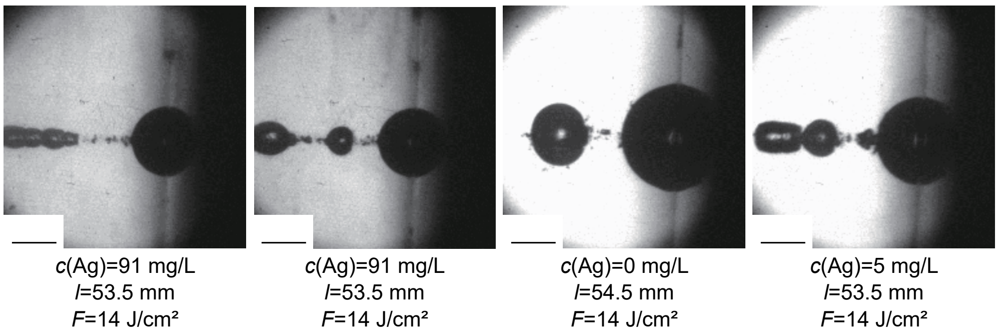

Fig. S3 | Bubble cascade images; the scale bars equal 250 μm. The experimental settings for each image are given below the respective image, where c(Ag) is the concentration of Ag NPs in the liquid, l is the focal distance, and F the fluence.

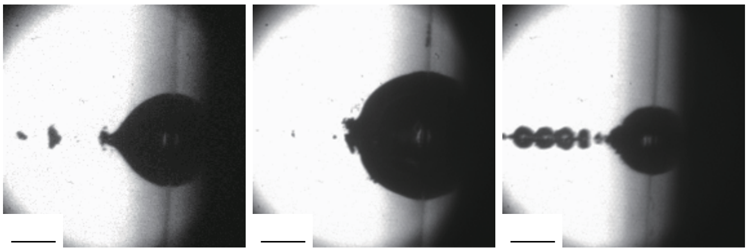

Fig. S4 | Cavitation bubble images, where spike- and ripple-like structures instead of hemispheres are observed; the scale bars equal 250 μm. The experimental settings for each image are given below the respective image, where c(Ag) is the concentration of Ag NPs in the liquid, *l* is the focal distance, and *F* the fluence.

Section 2: Calculation of flow parameter

Table S1 | Process and material (water) parameters for estimation of the flow condition in the ablation chamber

Title	Symbol	Value	Unit
Flow velocity	v	20	cm/min
Fluid density	ρ	1.0	g/cm³
Fluid dynamic viscosity	η	1.0	m(Pa·s)
Characteristic diameter	d	0.80	cm
Hydrodynamic NP radius	r	15	nm

Calculation of the s number Re results in laminar flow behavior

$$Re = \frac{\rho \cdot d \cdot v}{\eta} = 17 \tag{1}$$

Estimation of the diffusion coefficient of the NP D_{NP}

$$D_{NP} = \frac{k_B \cdot T}{6 \cdot \pi \cdot \eta \cdot r} = 1.5 \cdot 10^{-11}\ \mathrm{m^2/s} \tag{2}$$

Estimation of the mass transfer coefficient β for a spherical particle by the empirical equation[90]:

$$Sh = 1.6 \cdot Re^{0.54}$$
$$\beta = 1.6 \cdot \frac{D_{NP}}{2 \cdot r} \cdot \left(\frac{2 \cdot v \cdot r \cdot \rho}{\eta}\right)^{0.54} = 5.4 \cdot 10^{-6}\ \mathrm{m/s} \tag{3}$$

Calculation of the stationary layer thickness δ_c

$$\delta_c = \frac{D_{NP}}{\beta} = 2.7\ \mu\mathrm{m} \tag{4}$$

Since the NP distribution in the stationary layer is unknown, only the NP concentration in the completely mixed flow layer can be determined. With the values given in Table. S2, a concentration of about 3 μg/L, is calculated.

Table S2 | Process parameters for calculation of the NP concentration in the mixed flow layer

Title	value	Unit
Productivity per pulse	1	ng/pulse
Repetition rate	0.5	Hz
Flow rate	10	mL/min

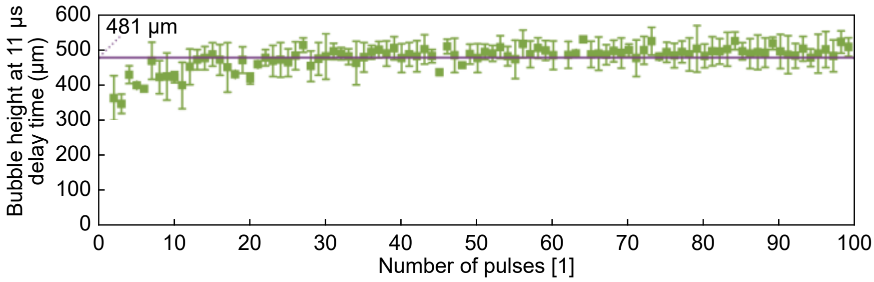

Fig. S5 | Cavitation bubble height at a delay time of 11 μs in dependency on the number of applied number of pulse on the same spot, the purple line presents the fit between 25 and 100 pulses.

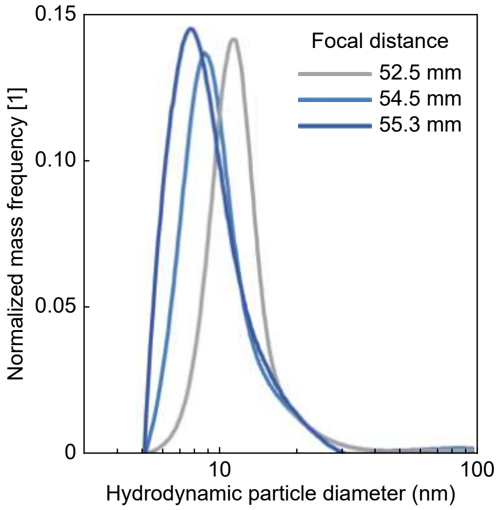

Fig. S6 | Mass-weighted, hydrodynamic size distribution measured by analytical disc centrifugation for Ag NPs at a focal distance of 52.5, 54.5, and 55.3 mm. The data are normalized so that the area under the curve equals 1.